

ELECTROCHEMICAL DEPOSITION OF HYDROUS RUTHENIUM OXIDE ON CONDUCTIVE DIAMOND FILMS AND ITS APPLICATION TO PHENOL OXIDATION IN ACIDIC MEDIA

Tanța SPĂȚARU*

Institute of Physical Chemistry “Ilie Murgulescu”, 202 Spl. Independenței, 060021, Bucharest, Romania

Received September 24, 2008

A new composite material was obtained by electrochemical deposition of hydrous ruthenium oxide ($\text{RuO}_x \cdot n\text{H}_2\text{O}$) particles on a boron-doped diamond (BDD) substrate. Cyclic voltammetry experiments have shown that $\text{RuO}_x \cdot n\text{H}_2\text{O}/\text{BDD}$ electrodes exhibit a large active area, high stability and promising electrocatalytic properties for phenol oxidation in acidic media. The possibility of using this electrode material for advanced phenol oxidation was also investigated. It was found that, unlike platinum or bare BDD, $\text{RuO}_x \cdot n\text{H}_2\text{O}/\text{BDD}$ is less sensitive to fouling and, at an applied potential of *ca.* 3.50 V, allows phenol oxidation ensuring a current efficiency as high as 35 %.

INTRODUCTION

Electrochemical treatment of wastewaters has recently attracted much interest, mainly because it ensures, at least in principle, an efficient treatment with no need for added chemicals. The use of the electrochemical technology in environmental engineering is a promising approach especially for the removal of organic pollutants that are usually resistant to biological treatment. Thus, the possibility exists for a particular organic compound to be oxidized, either at the electrode or by some electrochemically generated species (e.g. OH^\bullet , H_2O_2 , O_3).¹⁻³ Although the ideal treatment method is the “electrochemical combustion” that involves complete oxidation of the organic pollutant to CO_2 and H_2O , it should be noted that in some cases partial oxidation is also of interest. For example, it was found that in the case of phenols and their halogenated derivatives, partial electrochemical oxidation results in the formation of oxygenated functional groups or in the removal of one or several halogen atoms. Both these processes lead to an increase of the biological treatment efficiency.⁴

Extensive application of electrochemical wastewaters treatment relies upon finding suitable electrode materials that should have good

electrocatalytic activity, high chemical and electrochemical stability and should exhibit high overpotential for oxygen evolution in order to ensure reasonably good efficiency of the organic pollutant oxidation process. It is worth noting that the use of conventional electrode materials for the anodic treatment of organic wastes is limited, either by their low stability under severe working conditions (as in the case of graphite or glassy carbon), or by the fact that they are subject to fouling because the surface is blocked by reaction products or intermediates (as in the case of noble metals).⁵

Conductive diamond represents an electrode material that has attracted great interest due to its outstanding electrochemical features: wide potential window in aqueous solutions, low background current and inertness to adsorption.^{6,7} These unique properties, together with extreme robustness and high resistance to corrosion recommend polycrystalline diamond as an excellent electrode material, and its use for wastewater treatment is well substantiated.⁸ It was also found that the use of conductive diamond as a substrate for the deposition of metal oxide electrocatalysts results in high-activity deposits with excellent conductivity and negligible substrate effects.^{9,10} This allows the deposition of isolated particles, down to nanometer dimensions,

* Corresponding author: tspataru@icf.ro

or discontinuous films, thus maximizing the electrochemical utilization of the electrocatalyst by enhancing the active area of the electrode and by providing a large number of active sites in a small volume.

The present work was aimed at studying the electrochemical behavior of a composite material obtained by electrochemical deposition of hydrous ruthenium oxide ($\text{RuO}_x \cdot n\text{H}_2\text{O}$) on a boron-doped diamond (BDD) substrate, with an eye toward possible application for wastewater treatment. Preliminary results concerning phenol anodic oxidation on this electrode material are also reported.

RESULTS AND DISCUSSION

Fig. 1 shows cyclic voltammograms recorded during continuous $\text{RuO}_x \cdot n\text{H}_2\text{O}$ deposition on the BDD substrate. A well defined anodic peak with the peak potential of *ca.* 0.50 V (labeled I) was observed on the anodic branch of the voltammograms, followed by an increase of the deposition current at potential values higher than *ca.* 0.80 V. On the reverse scan two cathodic

peaks were evidenced (labeled II and III) with the peak potentials of *ca.* 0.80 and 0.10 V, respectively. The shape of the voltammograms in Fig. 1 is in line with previously reported data¹¹ suggesting that hydrous ruthenium oxide is formed within the range of peak I, while, at higher potential values further oxidation occurs to hydroxylated Ru(VI) species.

During the reverse scan these species are reduced back to $\text{RuO}_x \cdot n\text{H}_2\text{O}$ (peak II) and then to lower oxidation states. Peak III can be ascribed to the reduction of Ru(III) species and, within the same potential range, Ru metal and/or oxy-chlororuthenium compounds are deposited on the electrode surface. The oxidation of these deposited species during the following anodic scan enhances $\text{RuO}_x \cdot n\text{H}_2\text{O}$ formation. The slow increase of the deposition current within the potential range -0.20÷0.20 V shows that at the BDD surface the cathodic deposition of ruthenium species is a rather slow process, unlike the case of titanium substrate.¹¹ This behavior could be an advantage when aiming at obtaining isolated oxide particles because it allows a better control of the deposition process.

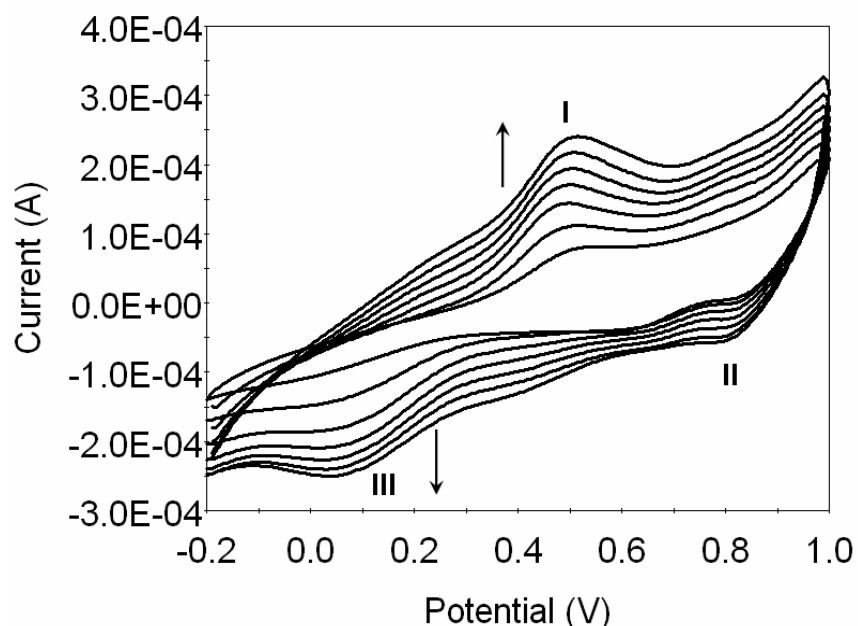


Fig. 1 – Voltammograms recorded during continuous $\text{RuO}_x \cdot n\text{H}_2\text{O}$ deposition on the BDD substrate, corresponding to deposition cycles no. 40, 60, 80, 100, 120, 140 and 160. The arrows indicate the increase of the number of deposition cycles. Electrolyte, 5 mM RuCl_3 + 0.1 M KCl + 0.01 M HCl ; scan rate, 50 mV s^{-1} .

After $\text{RuO}_x \cdot n\text{H}_2\text{O}$ deposition, the electrodes were soaked for 15 min in bidistilled water in order to remove from the surface undeposited ruthenium species. A typical scanning electron microscope (SEM) image obtained after ruthenium oxide

deposition (200 consecutive deposition cycles) on the BDD substrate is shown in Fig. 2. It can be observed that the deposit was discontinuous and rather nonuniform, with particle size ranging from *ca.* 200 – 600 nm.

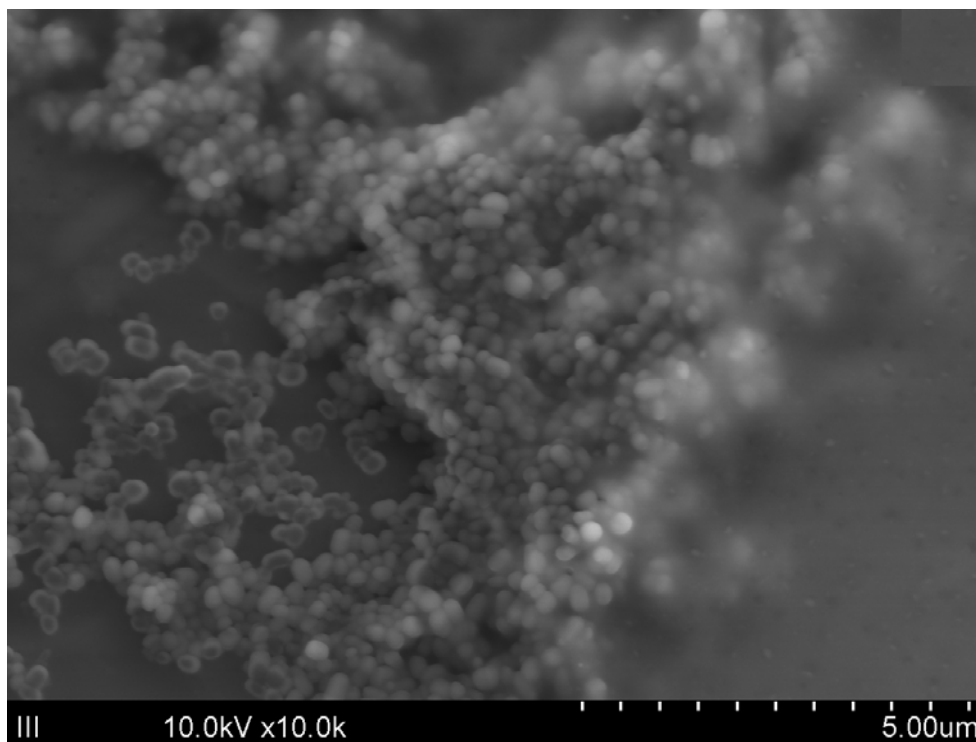


Fig. 2 – SEM image of the $\text{RuO}_x \cdot n\text{H}_2\text{O}$ deposited on the BDD substrate by 200 consecutive deposition cycles.

The electrochemical behavior of the electrode material thus obtained was checked by cyclic voltammetry (sweep rate, 20 mV s^{-1}) in a $0.5 \text{ M H}_2\text{SO}_4$ solution and the results are illustrated in Fig. 3. It was found that, after $\text{RuO}_x \cdot n\text{H}_2\text{O}$ deposition, the shape of the voltammogram (curve 2 in Fig. 3) is typical for the behavior of ruthenium

oxide in acidic media, the peaks occurring within the potential range $0.10 \div 1.00 \text{ V}$ being characteristic for the redox transitions in which Ru(III)/Ru(IV) species are involved.¹² It is clear that these redox processes at the electrode surface are highly reversible proving the good stability of the oxide deposit.

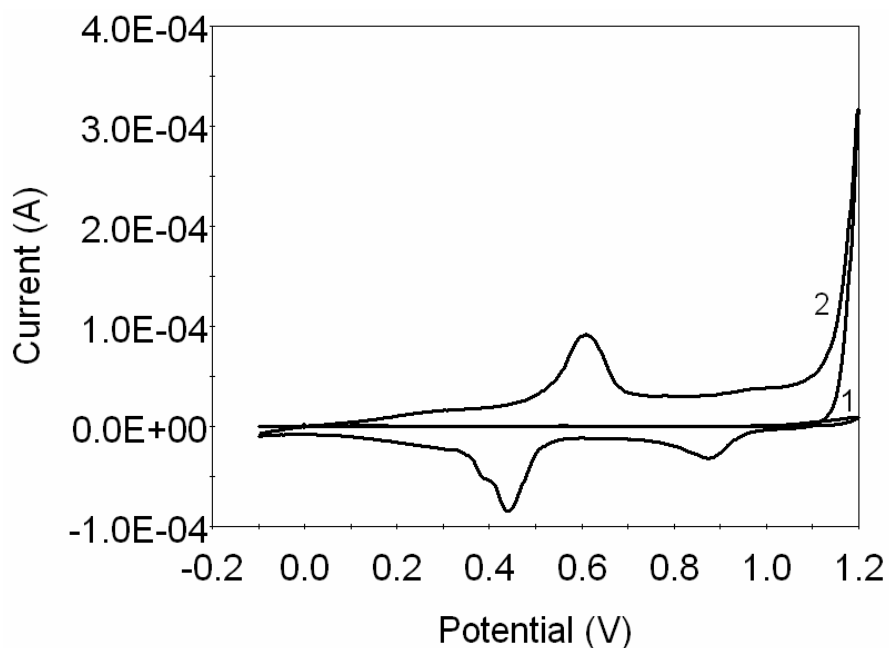
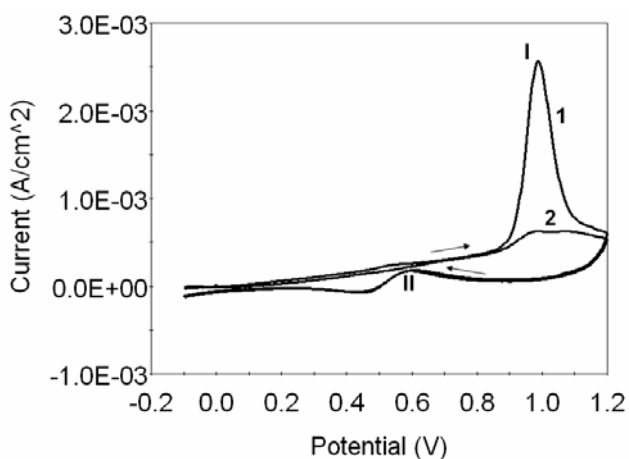


Fig. 3 – Cyclic voltammograms recorded at the BDD electrode before $\text{RuO}_x \cdot n\text{H}_2\text{O}$ deposition (1) and after 200 deposition cycles (2). Electrolyte, H_2SO_4 0.5 M ; scan rate, 20 mV s^{-1} .

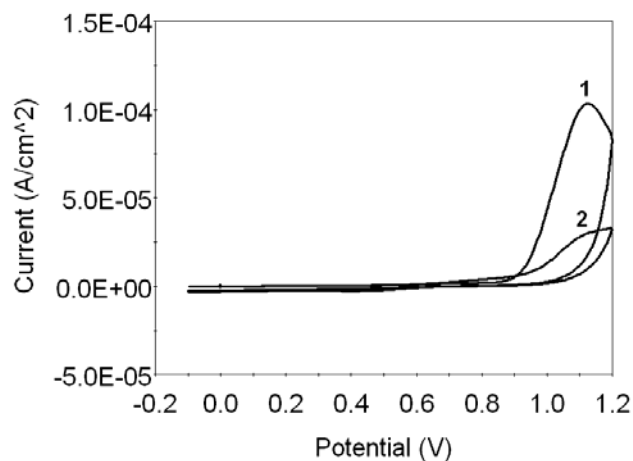
The significant enhancement of both reversible voltammetric charge and capacitive current is an indication of the presence of highly (although not uniformly) dispersed ruthenium oxide particles, in agreement with the results of the SEM measurements. The exponential increase of the oxygen evolution current at potential values higher than *ca.* 1.10 V is the result of the electrocatalytic properties of the oxide and put into evidence the fact that the electrochemical performances of the material are not affected by catalyst/substrate interactions.

In order to assess the use of $\text{RuO}_x \cdot n\text{H}_2\text{O}/\text{BDD}$ as electrode material for organic wastes oxidation, cyclic voltammetric experiments were performed in a 0.5 M H_2SO_4 + 10 mM phenol solution, at a sweep rate of 20 mV s^{-1} . A platinum working electrode and a bare BDD one were also used for comparison, and the results are shown in Fig. 4. It was found that at the Pt electrode (Fig. 4a) the first

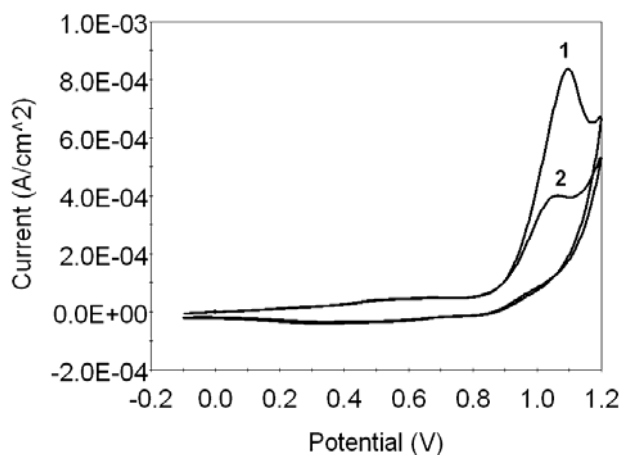
anodic scan results in the occurrence of a well defined peak (labeled I) with the peak potential of *ca.* 1.00 V. It is interesting to note that during the reverse scan, an additional anodic peak (II) appears at potential values close to 0.60 V. In order to understand the nature of this additional peak, one must take into account that during the first forward scan platinum oxidation takes place (prior to phenol oxidation), resulting in the formation of a thin platinum oxide film on the electrode surface. On the reverse scan, at potential values lower than *ca.* 0.80 V, platinum oxide reduction occurs and peak II can be therefore ascribed to the oxidation of phenol on the clean surface of the electrode. The small value of the current in the range of peak II suggests that, during the first anodic scan, the oxidation of the phenol results in the deactivation of the platinum electrode due to the fact that most of the active sites are blocked by the adsorption of some reaction products (presumably polyphenols).



a



b



c

Fig. 4 – Cyclic voltammograms recorded for phenol oxidation during the first (1) and the second scan (2) at Pt (a), BDD (b), and $\text{RuO}_x \cdot n\text{H}_2\text{O}/\text{BDD}$ electrode (c). Electrolyte, H_2SO_4 0.5 M + 10 mM phenol; scan rate, 20 mV s^{-1} .

Unlike platinum oxide, these compounds cannot be reduced during the reverse scan which leads to electrode fouling. Indeed, as curve 2 in Fig. 4a shows, during the second anodic cycle the current corresponding to phenol oxidation reaches only *ca.* 24 % of its initial value.

The same experiments performed by using a bare BDD working electrode showed that during phenol oxidation, this electrode material is also subject to fouling (although not to the same extent as the platinum), despite its well known inertness to adsorption.¹³ Thus, as Fig. 4b shows, the peak current for phenol oxidation during the second voltammetric cycle is *ca.* 36 % from the value recorded during the first scan.

Figure 4c shows characteristic voltammetric patterns recorded during phenol oxidation at electrodes obtained by $\text{RuO}_x \cdot n\text{H}_2\text{O}$ deposition (200 deposition cycles) on the BDD substrate. It was observed that oxide particles deposition resulted in a significant increase (*ca.* eight times) of the peak current during the first scan, compared to the case of the bare diamond (compare curves 1 from figures 4b and 4c). There are reasons to believe

that this behavior is mainly due to the enhancement of the active area induced by the deposition of hydrous ruthenium oxide. $\text{RuO}_x \cdot n\text{H}_2\text{O}$ deposition also resulted in a slight shift of the phenol oxidation peak toward lower potential values, supporting the conclusion that the oxide has an electrocatalytic effect for this process, although less significant than that of the platinum (Fig. 4a). The results illustrated in Fig. 4c are also noteworthy because they show that the composite material $\text{RuO}_x \cdot n\text{H}_2\text{O}/\text{BDD}$ is less sensitive to deactivation by polyphenol filming. Thus, a decrease of only *ca.* 50 % of the phenol oxidation peak current was observed in this case during the second voltammetric cycle.

Figure 5 shows polarization curves recorded at the $\text{RuO}_x \cdot n\text{H}_2\text{O}/\text{BDD}$ electrode (sweep rate, 5 mV s^{-1}) within the potential range $1.00 \div 4.00 \text{ V}$ in a stirred $0.5 \text{ M H}_2\text{SO}_4$ solution, both in the absence of phenol (curve 1) and in its presence (curve 2). The same experiments were carried out with a platinum electrode (surface area, 0.095 cm^2) and the results are shown in the inset from Fig. 5, for comparison.

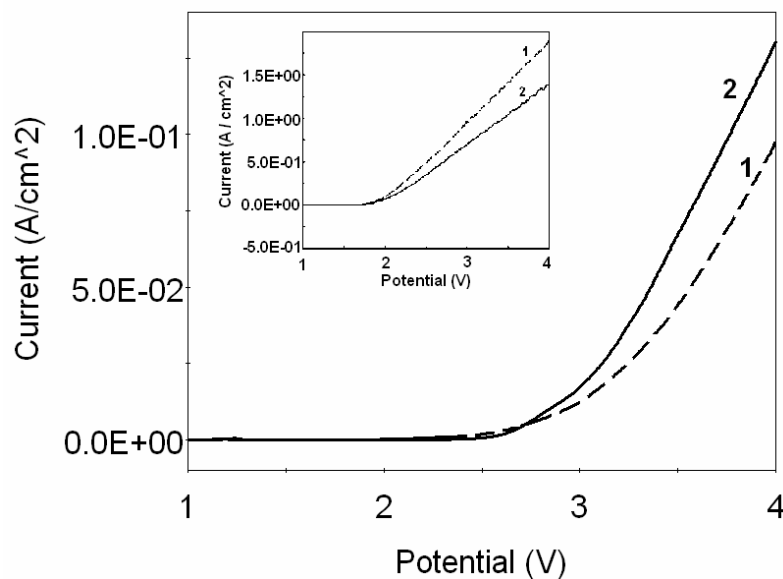


Fig. 5 – Polarization curves obtained at the $\text{RuO}_x \cdot n\text{H}_2\text{O}/\text{BDD}$ in a $0.5 \text{ M H}_2\text{SO}_4$ solution, in the absence of phenol (1) and at a concentration of 10 mM (2). Inset: results of the same experiment performed at Pt electrode. Scan rate, 5 mV s^{-1} .

It was observed that at the Pt electrode the presence of phenol (10 mM) results in a decrease of the anodic current over the whole of the investigated potential range (see the inset in Fig. 5). Therefore, it appears that the polymer films covering the electrode surface (which are formed at potential values close to *ca.* 1.00 V , as indicated by cyclic voltammetry experiments) are stable even at high anodic potentials, making platinum unsuitable for advanced phenol oxidation.

A different behavior was observed for $\text{RuO}_x \cdot n\text{H}_2\text{O}/\text{BDD}$ electrodes. Thus, as curve 2 from Fig. 5 indicates, within the potential range $2.00 \div 2.70 \text{ V}$ the anodic current in the presence of phenol is lower than that recorded in its absence. This is clearly the result of the polyphenol film presence. Nevertheless, starting from *ca.* 2.50 V the anodic current increases and its value surpasses that recorded in the background electrolyte. These findings support the conclusion that, unlike the

case of the Pt electrode, $\text{RuO}_x \cdot n\text{H}_2\text{O}/\text{BDD}$ could be used for advanced phenol oxidation, provided that the applied potential is high enough. A possible explanation for this behavior is provided by assuming that water molecules bound to the ruthenium oxide can be oxidized in one-electron step to produce $\text{Ru}-\text{OH}$ species that will assist in the further oxidation of phenoxy radicals (the primary oxidation products of the phenol) to benzoquinone.¹⁴ This could prevent, at least in

part, phenoxy radical polymerization which is known to be responsible for the deactivation of the electrode surface.

In order to put these results into a better perspective, the variation of the phenol oxidation current (calculated from Fig. 5 as the difference between the current in the presence and in the absence of phenol) as a function of the potential is shown in Fig. 6.

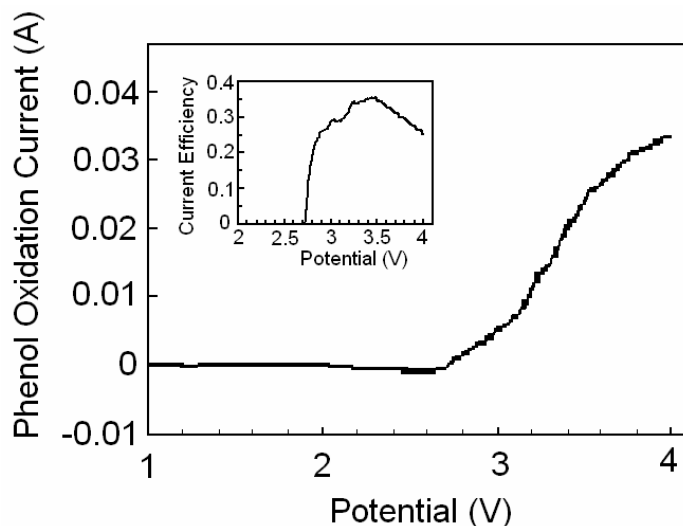


Fig. 6 – The variation of the phenol oxidation current at $\text{RuO}_x \cdot n\text{H}_2\text{O}/\text{BDD}$ electrodes, as a function of the potential. Inset: variation of the current efficiency for phenol oxidation at the $\text{RuO}_x \cdot n\text{H}_2\text{O}/\text{BDD}$ electrodes.

It can be observed that the oxidation of the polyphenol is a rather slow process that takes place within the potential range from *ca.* 2.60 to *ca.* 3.20 V. After the removal (perhaps only partial) of the film, the overall oxidation current is further increasing and tends to be diffusion-limited at potential values higher than *ca.* 3.60 V. The inset from Fig. 6 shows the variation of the current efficiency for phenol oxidation, calculated from the phenol oxidation current (Fig. 6) divided by the overall anodic current (curve 2 in Fig. 5). It appears that, at the $\text{RuO}_x \cdot n\text{H}_2\text{O}/\text{BDD}$ electrode, a value of the applied potential of *ca.* 3.50 V ensures a current efficiency for phenol oxidation of *ca.* 35 %. Further increase of the potential will result in a rather sharp decrease of the efficiency, due to strong oxygen evolution.

EXPERIMENTAL

The boron-doped polycrystalline diamond coatings were deposited on Si(111) wafers by means of microwave plasma-assisted chemical vapor deposition, in accordance with a previously described procedure.¹⁵ As in other works,¹⁶ hydrous ruthenium oxide was deposited by continuously cycling the potential of the electrode within the potential range

-0.10 to 1.00 V at a scan rate of 50 mV s^{-1} . The plating bath consisted of a 5 mM $\text{RuCl}_3 \cdot n\text{H}_2\text{O}$, 0.1 M KCl, and 0.01 M HCl aqueous solution. The measurements were performed in a conventional three-electrode glass cell at room temperature under ambient air. The exposed area of the working electrode was always 1.0 cm^2 and a platinum wire, together with an Ag/AgCl electrode were used as the counter electrode, and the reference electrode, respectively. All the substances were of analytical-reagent grade and all solutions were prepared with bidistilled water.

CONCLUSIONS

A new composite material was obtained by electrochemical deposition of hydrous ruthenium oxide particles (hundreds of nanometers in size) on a boron-doped polycrystalline diamond substrate. Cyclic voltammetry experiments have shown that $\text{RuO}_x \cdot n\text{H}_2\text{O}/\text{BDD}$ electrodes thus obtained exhibit a large active area, high stability and promising electrocatalytic properties for phenol oxidation in acidic media. These findings prompted us to investigate the possibility of using this electrode material for advanced phenol oxidation under steady-state conditions. It was observed that, unlike platinum or bare BDD, $\text{RuO}_x \cdot n\text{H}_2\text{O}/\text{BDD}$ is less sensitive to fouling and, at an applied potential

of ca. 3.50 V, allows phenol oxidation ensuring a current efficiency as high as 35 %.

Acknowledgments: This research was supported by the National Authority for Scientific Research (CEEEX project No. 309/2006).

REFERENCES

1. T. Matsue, M. Fujihara and T. Osa, *J. Electrochem. Soc.*, **1981**, *128*, 2565-2570.
2. P. Montilla, P. A. Michaud, E. Morallon, J. L. Vazquez and Ch. Comninellis, *Electrochimica Acta*, **2002**, *47*, 3509-3513.
3. C. Pîrvu, E. Brillas, O. Radovici and A. Banu, *Rev. Chim. (Bucharest)*, **2004**, *55*, 430-435.
4. M. Y. Rajashekharan, R. Jaganathan and R. V. Chaudhari, *Chem. Eng. Sci.*, **1998**, *53*, 787-792.
5. M. Panizza, P. A. Michaud, G. Cerisola and Ch. Comninellis, *Electrochem. Commun.*, **2001**, *3*, 336-342.
6. J. W. Strojek, M. C. Granger, T. Dallas, M. W. Holtz and G. M. Swain, *Anal. Chem.*, **1996**, *68*, 2031-2037.
7. T. N. Rao, I. Yagi, T. Miwa, D. A. Tryk and A. Fujishima, *Anal. Chem.*, **1999**, *71*, 2506-2511.
8. Ch. Comninellis, I. Duo, P. A. Michaud, B. Marselli and S. M. Park, in "Diamond Electrochemistry", A. Fujishima, Y. Einaga, T. N. Rao and D. A. Tryk (Eds.), Elsevier, Amsterdam, 2005, p. 449.
9. I. Duo, P. A. Michaud, W. Haenni, A. Perret and Ch. Comninellis, *Electrochem. Solid-State Lett.*, **2000**, *3*, 325-328.
10. N. Spătaru, K. Tokuhira, C. Terashima, T. N. Rao and A. Fujishima, *J. Appl. Electrochem.*, **2003**, *33*, 1205-1210.
11. C. C. Hu and Y. H. Huang, *J. Electrochem. Soc.*, **1999**, *146*, 2465-2471.
12. I. C. Stefan, Y. Mo, M. R. Antonio and D. A. Scherson, *J. Phys. Chem. B*, **2002**, *106*, 12373-12378.
13. A. Fujishima, Y. Einaga, T. N. Rao and D. A. Tryk, in "Diamond Electrochemistry", A. Fujishima, Y. Einaga, T. N. Rao and D. A. Tryk (Eds.), Elsevier, Amsterdam, 2005, p. 556.
14. S. Patra and N. Munichandraiah, *J. Electrochem. Soc.*, **2008**, *155*, F23-F27.
15. T. Yano, D. A. Tryk, K. Hashimoto and A. Fujishima, *J. Electrochem. Soc.*, **1998**, *145*, 1870-1876.
16. N. Spătaru, X. Zhang, T. Spătaru, D. A. Tryk and A. Fujishima, *J. Electrochem. Soc.*, **2008**, *155*, D73-D77.

